Materials and Methods

Reconfigurable hybrid interface for molecular marker diagnostics and in-situ reporting

Kristina Ehrhardt[a,c+], *Michael T. Guinn*[a,c+], *Tyler Quarton*[a,c], *Michael Q. Zhang*[a,c,d], *Leonidas Bleris*[a,b,c*]

[a]Bioengineering Department, The University of Texas at Dallas, 800 West Campbell Road, Richardson TX 75080 USA

[b]Electrical Engineering Department, The University of Texas at Dallas, 800 West Campbell Road, Richardson TX 75080 USA

[c]Center for Systems Biology, The University of Texas at Dallas, 800 West Campbell Road, Richardson TX 75080 USA

[d]Biological Sciences Department, The University of Texas at Dallas, 800 West Campbell Road, Richardson TX 75080 USA

*Corresponding author: Leonidas Bleris, The University of Texas at Dallas, NSERL 4.708, 800 West Campbell Road, Richardson TX 75080 USA

Email: bleris@utdallas.edu

Phone: 972-883-5785

+These two authors contributed equally

Supplementary Figures

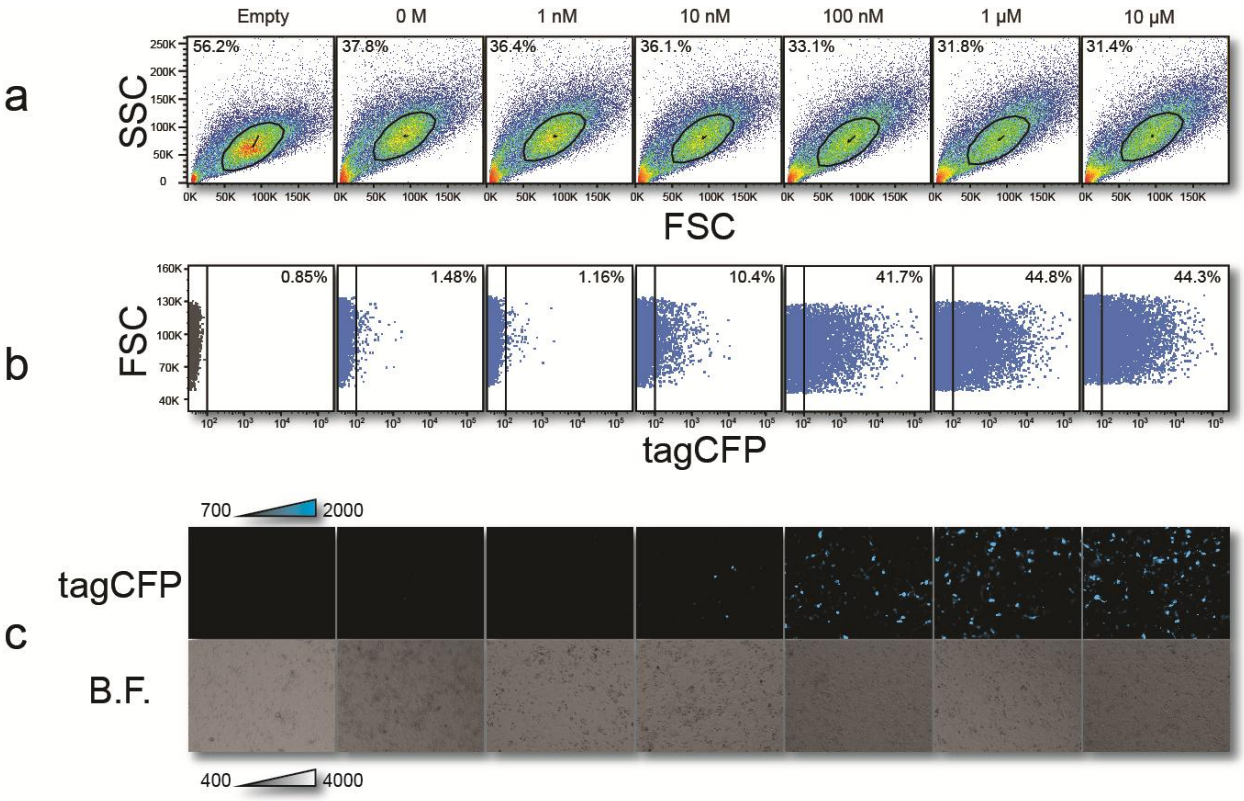

Supplementary Figure 1. Gating for AR Sensor induced with hydrocortisone. (a) Live cell gating of the AR sensor at different hydrocortisone concentrations. The gate was created based on the magnetic function within FlowJo. (b) TagCFP fluorescence gate based on empty cells (non-transfected). (c) Fluorescence microscopy of the AR sensor induced at different concentrations of hydrocortisone. Shown is both the TagCFP channel as well as the bright field.

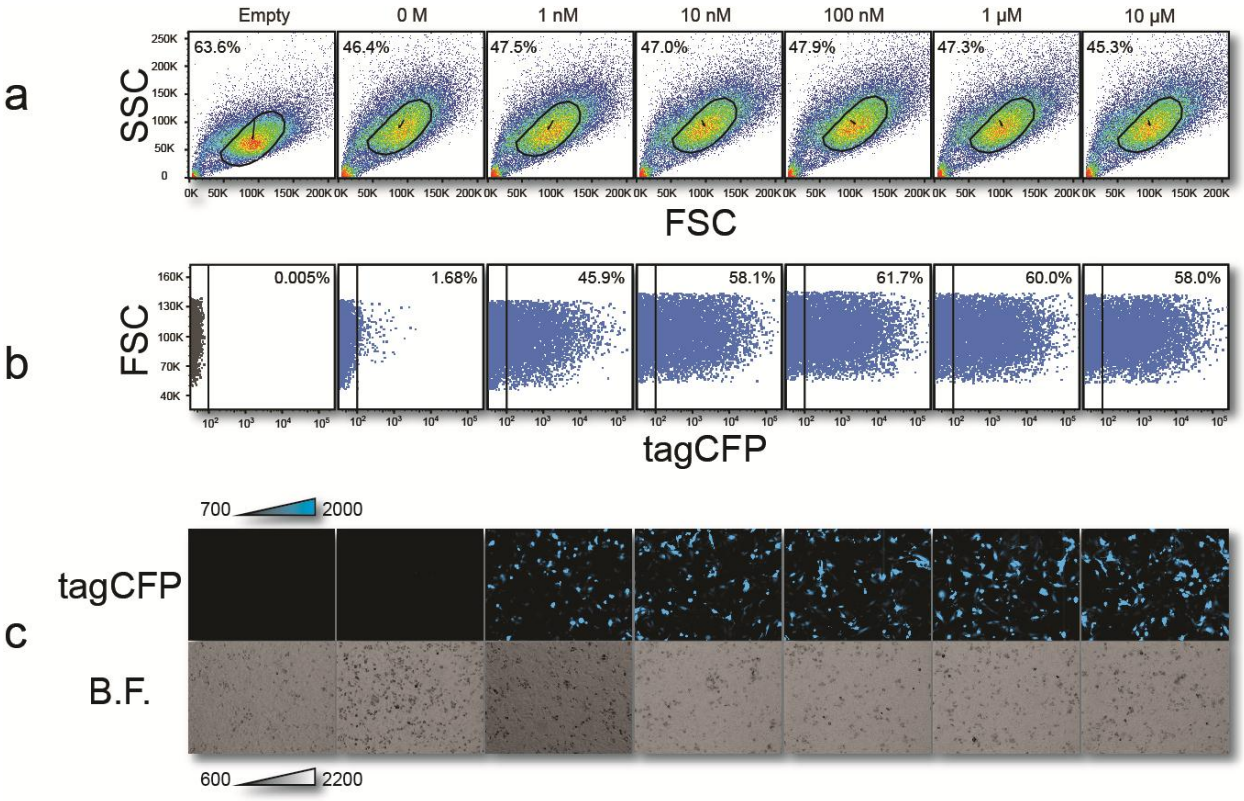

Supplementary Figure 2. Gating for AR Sensor induced with dexamethasone. (a) Live cell gating of the AR sensor at different dexamethasone concentrations. The gate was created based on the magnetic function within FlowJo. (b) TagCFP fluorescence gate based on empty cells (non-transfected). (c) Fluorescence microscopy of the AR sensor induced at different concentrations of dexamethasone. Shown is both the TagCFP channel as well as the bright field.

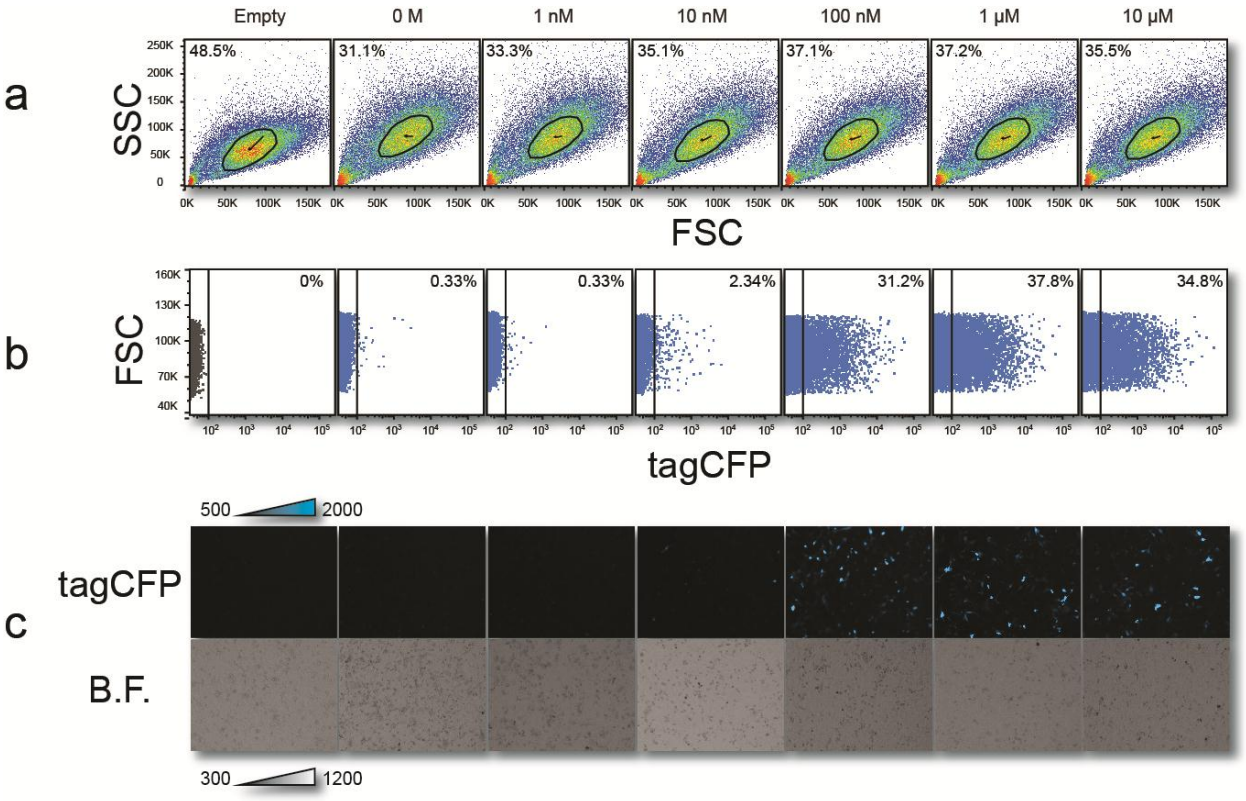

Supplementary Figure 3. Gating for GR Sensor induced with hydrocortisone. (a) Live cell gating of the GR sensor at different hydrocortisone concentrations. The gate was created based on the magnetic function within FlowJo. (b) TagCFP fluorescence gate based on empty cells (non-transfected). (c) Fluorescence microscopy of the GR sensor induced at different concentrations of hydrocortisone. Shown is both the TagCFP channel as well as the bright field.

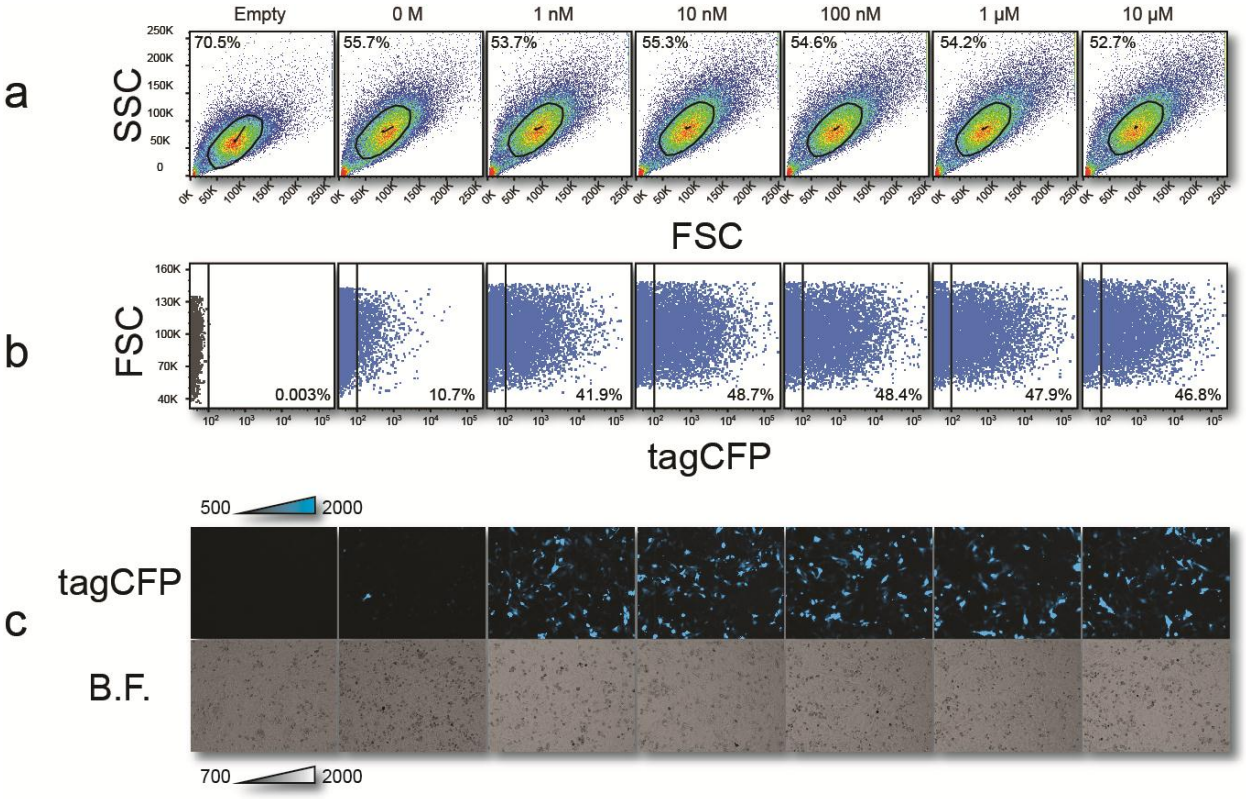

Supplementary Figure 4. Gating for GR Sensor induced with dexamethasone. (a) Live cell gating of the GR sensor at different dexamethasone concentrations. The gate was created based on the magnetic function within FlowJo. (b) TagCFP fluorescence gate based on empty cells (non-transfected). (c) Fluorescence microscopy of the GR sensor induced at different concentrations of dexamethasone. Shown is both the TagCFP channel as well as the bright field.

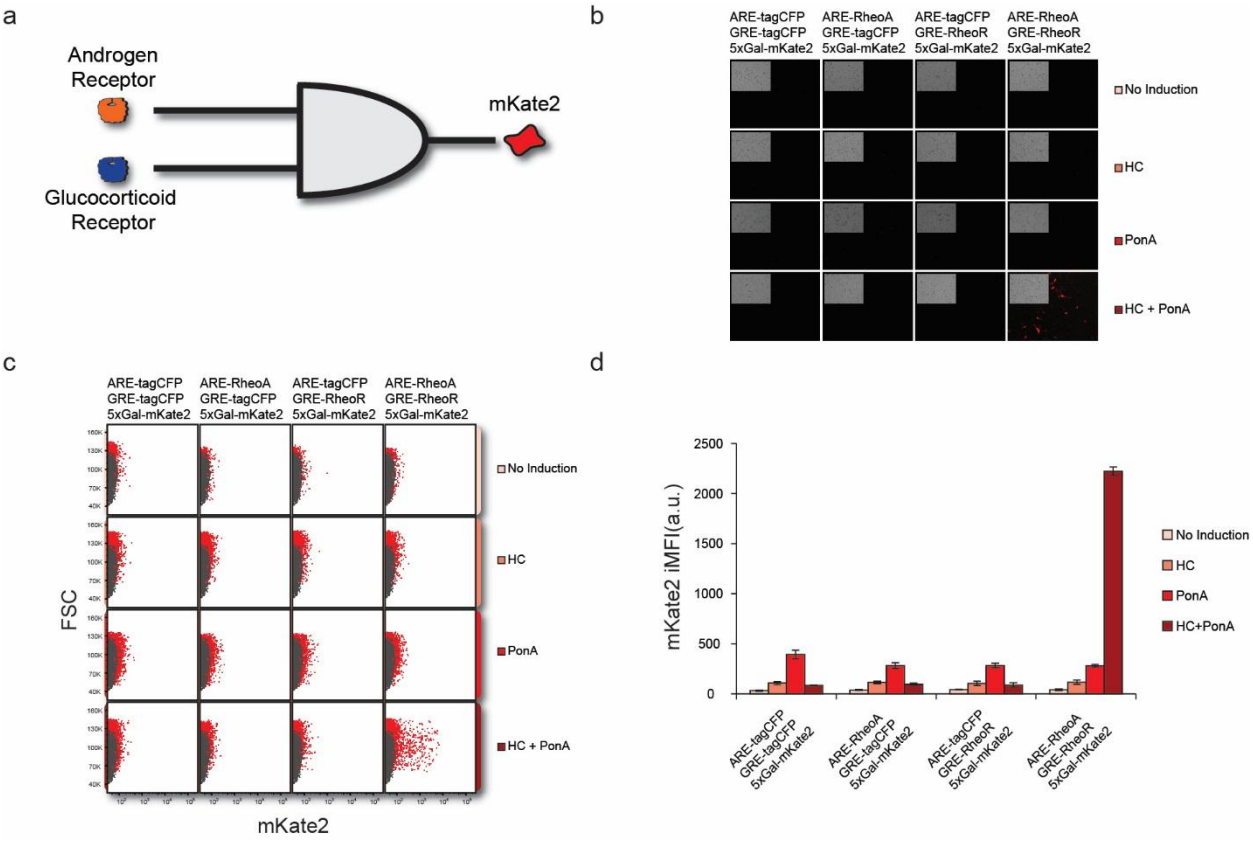

Supplementary Figure 5. Fan-in AND Gate controls. (a) Fan-in AND Gate schematic. (b) Fluorescence microscopy gate of Fan-in AND Gate under different induction and plasmid conditions. Both the bright field and mKate2 channel are shown for each case. (c) Flow cytometry scatter plots (Forward scatter versus mKate2) for the different induction and plasmid conditions. (d) mKate2 iMFI calculated from flow cytometry of the different induction and plasmid conditions.

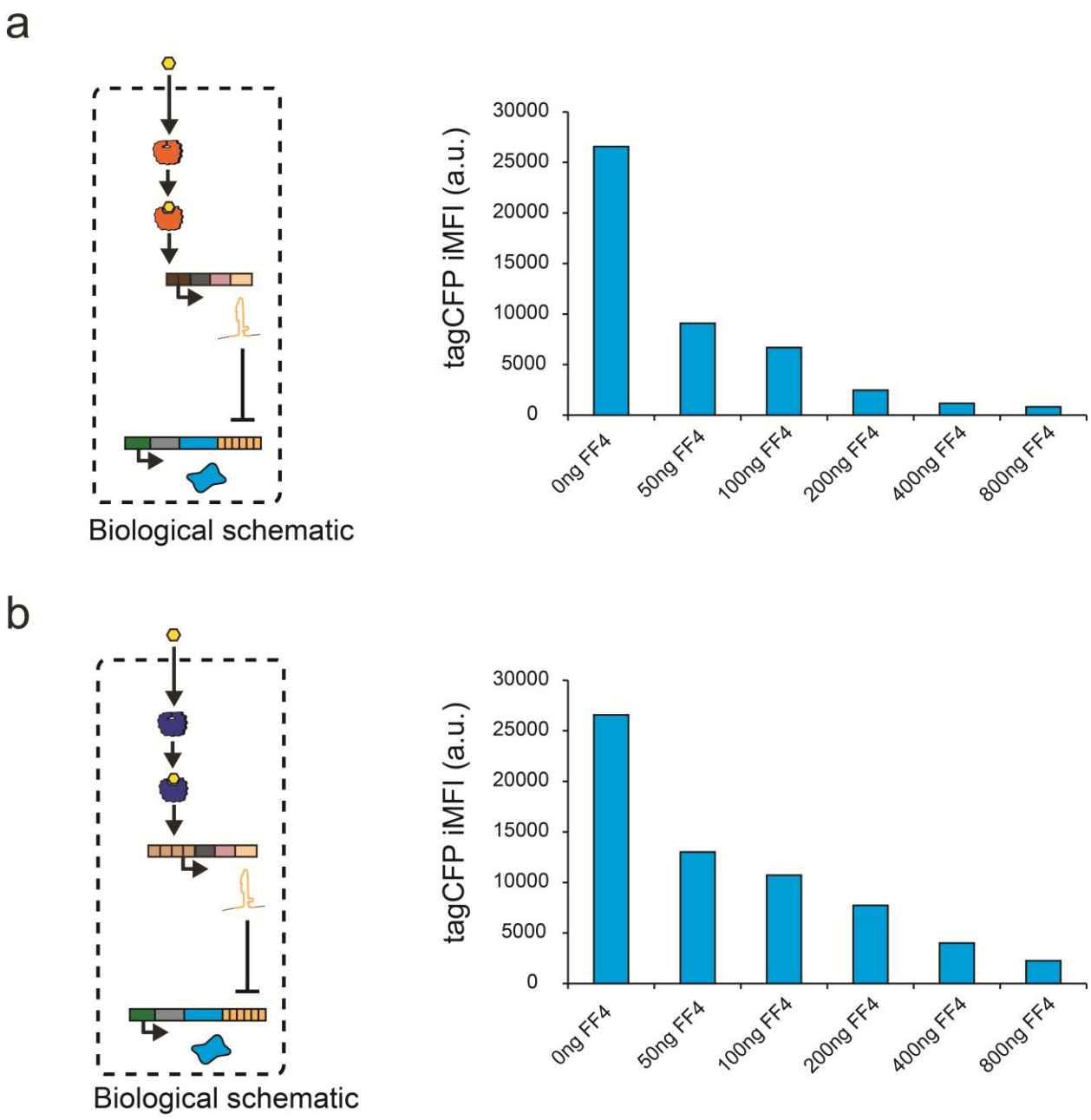

Supplementary Figure 6. Fan-in OR Gate optimization data. (a) Titration of ARE-CMV_{Min}-Neo-FF4 mass amounts on the UbC-TagCFP-FF3x3-FF4x3tgts. (b) Titration of GRE-CMV_{Min}-Neo-FF4 mass amounts on the UbC-TagCFP-FF3x3-FF4x3tgts.

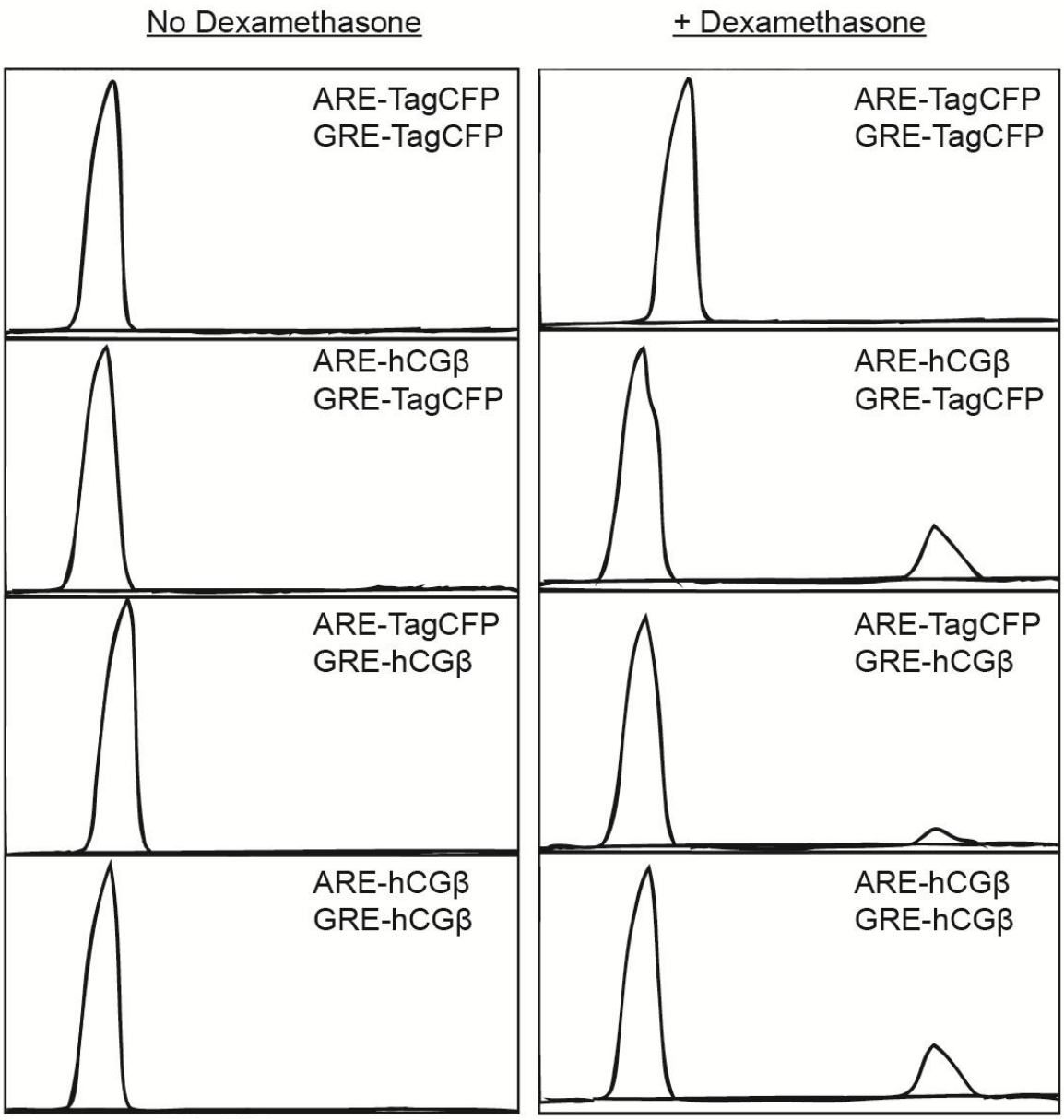

Supplementary Figure 7. Image-J Histograms of test strip control & test bands. Histograms generated by ImageJ of the test strip area where both the test band and control band appear.

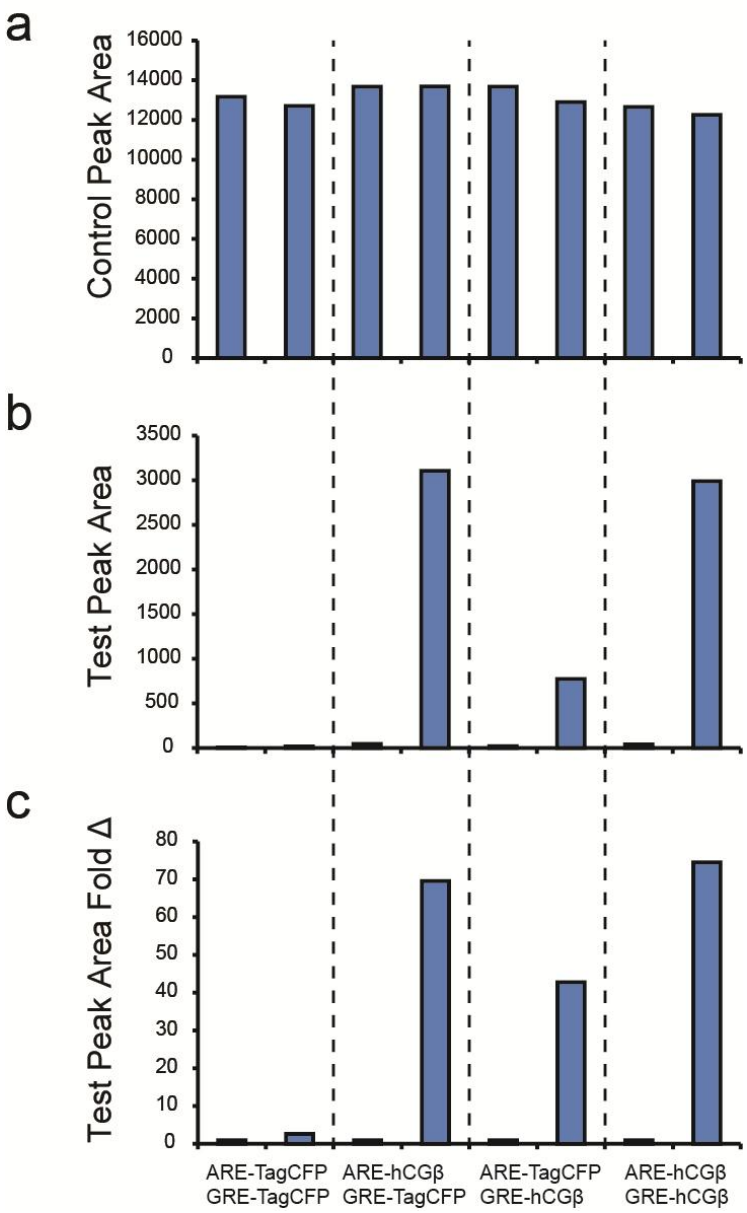

Supplementary Figure 8. Image-J Quantification of histograms of test strip control & test bands. (a) Relative control peak area calculated by ImageJ of the tall peaks shown in Supplementary Figure 7. (b) Relative test peak area calculated by ImageJ of the short peaks shown in Supplementary Figure 7. (c) Fold change of the test peak between each plasmid case; comparing the uninduced versus induced state.

Enzymes and reagents

Phusion DNA polymerase (Thermo Scientific, catalog number: F-530S), Q5 High-Fidelity DNA polymerase (New England Biolabs, catalog number: M0493S), and dNTPs (New England Biolabs, catalog number N0447S) were used in various PCR amplification reactions. Endonuclease restriction enzymes and T4 DNA Ligase (catalog number: M0202S) were purchased from New England Biolabs and used in digestion and ligation reactions respectively. Calf intestinal alkaline phosphatase (New England Biolabs, catalog number: M0290S) was used for de-phosphorylation reactions. Hydrocortisone (Alfa Aesar, #A16292), dexamethasone (Enzo Life Sciences, #BML-EI126-0001) and ponasterone A (Enzo Life Sciences, #ALX-370-014-M005) were used in the transfection of the genetic circuits within this work.

DNA purification was performed using Qiagen kits. For transformation, either competent DH5α cells (originally from Life Technologies, #18265-017), made using the standard $CaCl_2$ method of competent cell preparation, or high efficiency NEB5α competent cells (NEB, #C2987H) were used. All primers were synthesized by IDT or Sigma. All final plasmids were sequenced by Genewiz.

Recombinant DNA Constructs

CMV_{Min}: Equal molar (10µM final concentration) P1 and P2 were mixed in 1xT4 Polynucleotide kinase buffer (New England Biolabs, #M0201), heated to 95°C and slowly cooled down by 1°C/min to 25°C on a PCR block. 5uL of this was then mixed in ATP (final concentration 0.5 mM, New England Biolabs, #P0756) and T4 Polynucleotide kinase (final concentration 0.5 units/µL, New England Biolabs, #M0201) and the reaction was kept at 37°C for 30 min, ran on a 4% Metaphor agarose gel (Lonza, #50184) and then gel purified with the QIAquick Gel Extraction Kit (Qiagen, #28706). The minCMV sequence is 5'-TAGGCGTGTACGGTGGGAGGCCTATATAAGCAGAGCTCGTTTAGTGAACCGTCAGA TCGC-3'.

ARE-CMV_{Min}-TagCFP and GRE-CMV_{Min}-TagCFP: pAR-luc and pGR-luc were purchased from Panomics (#LR0007, and #LR0033) and pTagCFP-N was purchased from Evrogen (#FP112). The above insert (minCMV) was cloned into pAR-luc and pGR-luc using BglII and HindIII sites. TagCFP was PCR amplified from pTagCFP-N using primers P3 and P4 and cloned into pAR-minCMV-luc and pGR-minCMV-luc using FseI and HindIII sites.

ARE-CMV_{Min}-RheoActivator: The RheoSwitch Mammalian Inducible Expression System (pNEBR-R1) was purchased from New England Biolabs (#E3000). The RheoActivator was PCR amplified from pNEBR-R1 using primers P5 and P6 and cloned into ARE-minCMV-TagCFP using HindIII and FseI sites.

GRE-CMV$_{Min}$-RheoReceptor: The RheoReceptor was PCR amplified from pNEBR-R1 using primers P7 and P8 and cloned into GRE-minCMV-TagCFP using HindIII and FseI sites.

ARE-minCMV-Neo-FF4 and GRE-minCMV-Neo-FF4: Neo-FF4 was PCR amplified from p234-CMV-Neo-FF4 from Leisner et al using primers P9 and P10 and cloned into ARE-minCMV-TagCFP and GRE-minCMV-TagCFP using HindIII and FseI sites (Leisner et al., 2010).

UbC-(LacOx2)-TagCFP-pest-F4x3: See Guinn et al (Guinn and Bleris, 2014).

5xGal-mKate2: pmKate2-C was purchased from Evrogen (#FP322) and pNEB-X1 Hygro from New England Biolabs. MKate2 was PCR amplified from pmKate2-C using primers P11 and P12 and cloned into 5xgal (pNEB-X1) using NheI and HindIII sites.

pTAL1- TALE$_{ARE}$-KRAB: The TALE construct was prepared using the Golden Gate TALEN and TAL effector kit (Addgene, #1000000016) developed by Cermak et al (Cermak et al., 2011). The TAL effector target sequence and its according RVD sequence were designed using the online tool TAL Effector Targeter (Doyle et al., 2012). The target sequence is ACCGAGCTCTTACGCG. The pTAL1-KRAB plasmid from Yi et al was used (Li et al., 2012).

Ef1α-ARE-TALE_KRAB: The TALE was digested from the pTAL1 plasmid and cloned into the EF1 vector from Yi et al using EcoRI sites (Li et al., 2012).

Ef1α-TALE$_{ARE}$-KRAB-F4x3-F3x3: The DNA binding domain of EF1α-TALE$_{ARE}$-VP16 vector (unpublished vector) was digested out with BssHII & AatII and cloned into the EF1α-TALE$_{UbC}$-FF3x3-FF4x3tgts (from Li et al reference) vector with the same enzymes.

Ef1a-TALE$_{ARE}$-KRAB-miR21tgtsx4: The TALE$_{ARE}$-KRAB was PCR amplified from Ef1a-TALE$_{ARE}$-KRAB-miR21tgtsx4 using primers P15 & P16 to generate TALE$_{ARE}$-KRAB-miR-21x4tgts. This fragment was then cloned into Ef1a-TALE$_{ARE}$-KRAB-miR21tgtsx4 using AatII & NotI restriction enzymes.

ARE- CMV$_{min}$-hCGβ and GRE- CMV$_{min}$-hCGβ: HCGβ was PCR amplified from Open Biosystems hCG vector (Catalog number: MHS1768-9143756) using primers P17 and P18 and cloned into ARE-minCMV-TagCFP and GRE-minCMV-TagCFP using HindIII and FseI.

Primer List

Primer ID	Primer Sequence	Function
P1	GATCTTAGGCGTGTACGGTGGGAGGCCTATATAAGCAGAG CTCGTTTAGTGAACCGTCAGATCGCA	for minCMV
P2	AGCTTGCGATCTGACGGTTCACTAAACGAGCTCTGCTTATAT AGGCCTCCCACCGTACACGCCTAA	for minCMV
P3	ATCAAGCTTCGCTACCGGTCGCCACCAT	Forward primer for TagCFP
P4	CCAGGCCGGCCTTAGCGGTACAGCTCGTCCA	Reverse primer for TagCFP
P5	CCAAAGCTTATGGGCCCTAAAAAGAAGC	Forward primer for RheoActivator
P6	CCAGGCCGGCCTTATGAATCAGAAGGTGATT	Reverse primer for RheoActivator
P7	CCAAAGCTTATGAAGCTACTGTCTTCTATCG	Forward primer for RheoReceptor
P8	CCAGGCCGGCCCTAGAGATTCGTGGGGGACTC	Reverse primer for RheoReceptor
P9	CCAAAGCTTATGGGATCGGCCATTGAAC	Forward primer for Neo-FF4
P10	CCAGGCCGGCCGAAGTGATCTTCCGTCACAGG	Reverse primer for Neo-FF4
P11	CCAGTAGCTAGCATGGTGAGCGAGCTGATTAAGGAGAACA	Forward primer for mKate
P12	CCAGTAAAGCTTTCTGTGCCCCAGTTTGCTAGGGAGG	Reverse primer for mKate
P13	CCAACGCGTACCGCCATGCATTAGTTAT	Forward primer for CMV-TagCFP
P14	CCAACGCGTTTAGCGGTACAGCTCGTCCA	Reverse primer for CMV-TagCFP
P15	CAGTACgacgtcctgccatggatgca	Forward TALE(ARE)-KRAB
P16	CAGTACgcggccgcTAGCTTATCAGACTGATGTTGATAGCTTA TCAGACTGATGTTGATAGCTTATCAGACTGATGTTGATAGCT TATCAGACTGATGTTGAggtaccgtcgactgcaga	Reverse TALE(ARE)-KRAB to add miR-21 tgts
P17	CCAAAGCTTatggagatgttccaggggct	Forward primer for hCGβ
P18	CCAGGCCGGCCttattgtgggaggatcgggg	Reverse primer for hCGβ

Biological Parts

Biological Component	Description
EF1α	The human elongation factor-1 alpha promoter which causes strong constitutive transcription of the gene downstream.
Androgen Response Operator	A DNA sequence that consists of 2 repeats of the 23 base pair sequence that is bound by the androgen receptor. When the androgen receptor binds this site, transcription of the downstream gene is driven.
Glucocorticoid Respone Operator	A DNA sequence that consists of 4 repeats of the 15 base pair sequence that is bound by the glucocorticoud receptor. When the glucocorticoid receptor binds this site, transcription of the downstream gene is driven.
Androgen Receptor	The human transcription factor that binds the androgen response operator sequence.
Glucocorticoid Receptor	The human transcription factor that binds the glucocorticoid response operator sequence.
Rheo Activator (RheoA)	An insect/mammalian RXR hybrid protein that is fused to the viral activation domain VP16. This protein dimerizes with the RheoR, which can subsequently bind the 5xGal operator to drive downstream gene expression.
Rheo Receptor (RheoR)	An insect nuclear receptor fused to the yeast GAL4 DNA binding domain. This protein dimerizes with the RheoA, which can subsequently bind the 5xGal operator to drive downstream gene expression.
5xGal operator	A DNA sequence that consists of 5 repeats of the 24 base pair sequence that is bound by the RheoA-RheoR complex. When the RheoA-RheoR complex binds this site, transcription of the downstream gene is driven.
human chorionic gonadotropin beta (hCGβ)	A human hormone peptide produced endogenously only when an ovum is fertilized by a sperm.
Neomycin resistant gene	A gene used for the purpose of creating the synthetic microRNA FF4.
TALE-KRAB	A DNA-binding protein fused with the Krüppel associated box (KRAB) that binds a sequence of the androgen response element, therefore preventing transcription of the gene downstream.
KRAB	The Krüppel associated box (KRAB) is a transcriptional repression domain.
Hydrocortisone (HC)	A molecular hormone that binds to both the androgen receptor and glucocorticoud receptor. Upon binding these hormones, the hormones translocate into the nucleus.
Dexamethasone (Dex)	A synthetic hormone that binds to both the androgen receptor and glucocorticoud receptor. Upon binding these hormones, the hormones translocate into the nucleus.
Ponasterone (PonA)	An analog of the insect hormone Ecdysone, which causes dimerization of the RheoA & RheoR proteins, leading to binding of the 5xGal operator and downstream gene expression.

CMVmin	A 59 nucleotide sequence of CMV promoter sequence that only drives gene transcription when the adjacent enhancer region is bound by the activating transcription factor.
tagCFP	Cyan Fluorescent Protein.
mKate2	Far-red Fluorescent Protein.
miR-FF4	A synthetic microRNA produced from miR-30.
FF4X3tgts	Perfect complimentary microRNA targets that the synthetic microRNA miR-FF4 bind.
miR21x4tgts	Perfect complimentary microRNA targets that the endogenous microRNA miR-21 bind.

Experimental Table

	DNA Transfected	Transient Transfection	Transfection Reagent	Flow Cytometer
Figure 1a-c Supplement Figure 1 & 2	500ng GRE-CMVmin-TagCFP plasmid 500ng Junk plasmid	~250,000 cell per well	JetPrime®(2.4 µl & 75 µl buffer) per well	TagCFP: 240 V
Figure 1d-f Supplement Figure 3 & 4	500ng ARE-CMVmin-TagCFP plasmid 500ng Junk plasmid	~250,000 cell per well	JetPrime®(2.4 µl & 75 µl buffer) per well	TagCFP: 240 V
Figure 2	500ng ARE-CMVmin-TagCFP plasmid 500ng Junk plasmid 500ng ARE-CMVmin-TagCFP plasmid 500ng EF1α-TALE(ARE)-FF3x3-FF4x3tgts 500ng ARE-CMVmin-TagCFP plasmid 500ng EF1α-TALE(ARE)-miR-21x4tgts	~250,000 cell per well	JetPrime®(2.4 µl & 75 µl buffer) per well	TagCFP: 240 V
Figure 3a-c	250ng ARE-CMVmin-RheoA 250ng GRE-CMVmin-RheoR 250ng 5xGal-CMVmin-mKate2	~250,000 cell per well	JetPrime®(2.4 µl & 75 µl buffer) per well	mKate2: 320 V
Figure 3d-f	250ng UbC-LacOx2-TagCFP-FF3x3-FF4x3tgts 800ng ARE-CMVmin-FF4 plasmid 800ng GRE-CMVmin-RheoR plasmid 250ng UbC-LacOx2-TagCFP-FF3x3-FF4x3tgts 500ng ARE-CMVmin-FF4 plasmid 500ng GRE-CMVmin-FF4 plasmid 250ng UbC-LacOx2-TagCFP-FF3x3-FF4x3tgts 500ng ARE-CMVmin-FF4 plasmid 500ng GRE-CMVmin-FF4 plasmid	~250,000 cell per well	JetPrime®(2.4 µl & 75 µl buffer) per well	TagCFP: 240 V
Figure 4	10µg ARE-CMVmin-hCGβ plasmid 10µg GRE-CMVmin-TagCFP plasmid 10µg ARE-CMVmin-TagCFP plasmid 10µg GRE-CMVmin-hCGβ plasmid 10µg ARE-CMVmin-hCGβ plasmid 10µg GRE-CMVmin-hCGβ plasmid	~250,000 cell per well	JetPrime®(24 µl & 750 µl buffer) per plate	N/A

References

Cermak, T., Doyle, E.L., Christian, M., Wang, L., Zhang, Y., Schmidt, C., Baller, J.A., Somia, N.V., Bogdanove, A.J., Voytas, D.F., 2011. Nucleic Acids Res. 39, e82-e82.

Doyle, E.L., Booher, N.J., Standage, D.S., Voytas, D.F., Brendel, V.P., VanDyk, J.K., Bogdanove, A.J., 2012. Nucleic Acids Res. 40, W117-W122.

Guinn, M., Bleris, L., 2014. ACS synthetic biology. 3, 627-633.

Leisner, M., Bleris, L., Lohmueller, J., Xie, Z., Benenson, Y., 2010. Nature nanotechnology. 813, 169-186.

Li, Y., Moore, R., Guinn, M., Bleris, L., 2012. Scientific reports. 2.